A novel wide measuring range FBG displacement sensor with variable measurement precision based on helical bevel gear*

JIANG Shan-chao (蒋善超), **WANG Jing** (王静)**, **SUI Qing-mei** (隋青美), **and CAO Yu-qiang** (曹玉强)
Optical Fiber Sensing Technology and Engineering Research Center, Shandong University, Jinan 250061, China

(Received 29 September 2014; Revised 7 November 2014)

A novel fiber Bragg grating (FBG) displacement sensor is proposed, which can achieve wide measuring range displacement detection with variable measurement precision due to its mechanical transfer structure of helical bevel gear. A prototype is designed and fabricated. The maximum detection displacement of this prototype is 1.751 m, and the precision grade changes from 0.2% to 6.7%. Through analyzing the experiment data which is obtained in the calibration experiment, the measuring range of this sensor is from 0 m to 1.532 m, and the wavelength shift errors between experiment data and theory calculation are all less than 5%.

Document code: A **Article ID:** 1673-1905(2015)02-0081-3
DOI 10.1007/s11801-015-4176-1

Many existing displacement measurement methods, such as inductance, capacity, photoelectric and ultrasonic displacement sensors, are difficult to do waterproof and achieve stable monitoring[1-5]. Due to their unique advantages, fiber Bragg grating (FBG) displacement sensors have been widely investigated[6-10]. While the measuring ranges of existing FBG displacement sensors are mostly at centimeter magnitude which are limited by material properties of FBG or sensor structure. Yi Zou et al[11] proposed an FBG displacement sensor with measuring range of 0–10 mm. Such a measuring range greatly limits the application of FBG displacement sensor in large-scale structure health monitoring. In order to achieve the wide measuring range and the high monitoring precision at small displacement range, a novel FBG displacement sensor with variable measurement precision based on helical bevel gear[12,13] is designed and fabricated in this paper.

Fig.1 shows the design diagram and the prototype of the metal transfer structure in this novel FBG displacement sensor. Due to the changing radius along its axis, the relationship between circumferential length $L_{a\to b}$ from point a to point b and radian θ is not linear, which is expressed as

$$L_{a\to b}=\int_0^{\theta}(r+\frac{R-r}{n}\cdot\frac{x}{2\pi})\mathrm{d}x=(r+\frac{R-r}{n}\cdot\frac{\theta}{2\pi})\theta, \tag{1}$$

where n is thread turns number on the gear, and $L_{a\to b}$ represents the external displacement which is needed to be detected.

With the same radian of θ, the circumferential length L_g of groove with width of d is

$$L_g=r_1\cdot\theta, \tag{2}$$

so the relationship between $L_{a\to b}$ and L_g can be expressed as

$$L_{a\to b}=(r+\frac{R-r}{n}\cdot\frac{L_g}{2\pi r_1})\cdot\frac{L_g}{r_1}. \tag{3}$$

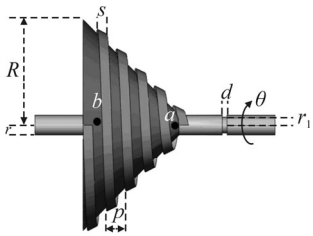

(a)

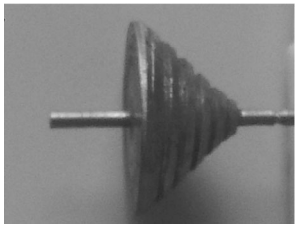

(b)

Fig.1 (a) Design diagram and (b) prototype of the metal transfer structure

* This work has been supported by the National Natural Science Foundation of China (Nos.61174018, 41472260 and 41202206).
** E-mail: wangjing329@mail.sdu.edu.cn

As the geometric parameters of helical bevel gear are determinate, $L_{a\to b}$ changes faster and faster following L_g. Basic geometric parameters of the gear are exhibited in Tab.1.

Tab.1 Geometric parameters of helical bevel gear

Index	R	r	r_1	n
Value/mm	21.5	2	1.5	5

Theoretical calculation model of this novel FBG displacement sensor is displayed in Fig.2.

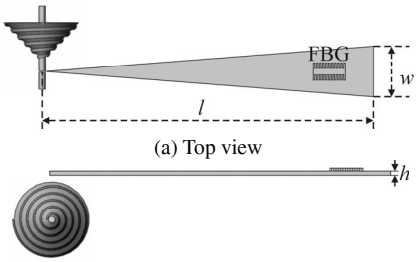

(a) Top view

(b) Front view

Fig.2 Theoretical calculation model of the novel FBG displacement sensor

As shown in the calculation model, the circumferential length L_g is free end deflection of the triangle cantilever beam. The relationship between deflection L_g and surface strain ε of cantilever beam is

$$L_g = \frac{l^2}{h}\cdot\varepsilon\ . \tag{4}$$

The FBG as a core sensitive element has wavelength selection characteristics, and only those wavelengths which satisfy the Bragg condition are affected and strongly back-reflected. The reflected center wavelength can be expressed as[15]

$$\lambda_B = 2n_{eff}\Lambda\ , \tag{5}$$

where n_{eff} is the effective index of refraction, and Λ is the grating periodicity of the FBG.

Due to the influence of temperature and strain on parameters of n_{eff} and Λ, the reflected wavelength is changed as a function of temperature and strain. Keeping the temperature stable, the general relationship between strain and wavelength can be described as[16,17]

$$\frac{\Delta\lambda_B}{\lambda_B} = (1-p_e)\varepsilon\ , \tag{6}$$

where λ_B and p_e are center wavelength and optical elasticity coefficient, respectively.

So the relationship between the detected displacement and center wavelength shift is

$$L_{a\to b} = (r+\frac{R-r}{n}\cdot\frac{K\cdot\Delta\lambda_B}{2\pi r_1})\cdot\frac{K\cdot\Delta\lambda_B}{r_1}\ , \tag{7}$$

where K is the coefficient between deflection and center wavelength shift obtained from Eqs.(4) and (6), and it is expressed as

$$K = \frac{l^2}{h\cdot\lambda_B\cdot(1-p_e)}\ . \tag{8}$$

When the basic parameters of this novel FBG sensor, such as geometric parameters of metal transfer instrument and triangle cantilever beam and physical coefficient of FBG, are identified, the external displacement can be expressed as a quadratic equation of center wavelength shift. The length and height of cantilever beam are 100 mm and 1 mm, respectively. The initial center wavelength of FBG is 1 550.220 6 nm, and p_e is equal to 0.22[18,19]. Assuming that maximum center wavelength shift is 8 nm, and the detected displacement ranges are calculated as 0–1.751 m, the theoretical calculation formula between $L_{a\to b}$ and $\Delta\lambda_B$ under the same conditions is

$$L_{a\to b} = 19.772\cdot\Delta\lambda_B^2 + 60.662\cdot\Delta\lambda_B\ . \tag{9}$$

To verify the performance of this novel FBG displacement sensor practically, the calibration experiment platform as shown in Fig.3 is built up based on SM125[20] as the fiber integrator, displacement platform and data acquirement software.

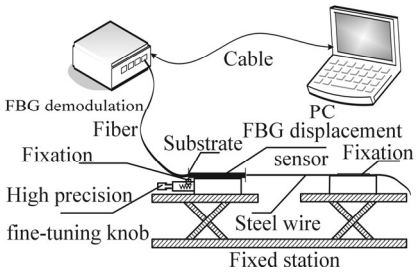

Fig.3 Schematic diagram of the displacement sensor calibration platform

Through adjusting the high precision fine-tuning knob with stepping accuracy of 1 mm, the external displacement is changed from 0 mm to 150 mm. This maximum detection displacement of 150 mm is limited by the calibration platform. The initial center wavelength of the FBG pasted on the cantilever is the same as that in the calculation model. To make sure that the FBG reflectance spectrum is not widened, the wavelength shift ranges in this experiment are manually controlled within 0–1.5 nm. Varying precision grade is chosen as the reference index to evaluate the performance of this novel FBG sensor, and is expressed as

$$G = \frac{L_{a\to b}(\Delta\lambda_B + 1\ \text{pm}) - L_{a\to b}(\Delta\lambda_B)}{L_{a\to b}(\Delta\lambda_B)}\ . \tag{10}$$

Fig.4 displays the wavelength shift and the measurement precision grade versus external displacements. The formula of the fitting curve between external displacement $L_{a\to b}$ (mm) and wavelength shift $\Delta\lambda_B$ (nm) of the prototype in the calibration experiment is

$$L_{a\to b} = 16.527 \cdot \Delta\lambda_B^2 + 59.280 \cdot \Delta\lambda_B - 0.255\ 8, \qquad (11)$$

and the linearity of approximate formula is R^2=0.999 7. Assuming that $\Delta\lambda_B$ is 8 nm, the maximum measuring displacement of the prototype is 1.532 m practically. It is shown in Fig.4 that the smaller the detected displacement, the higher the precision grade. The measurement precision grade decreases with the increase of detected displacement. When the external displacement is larger than 50 mm, the precision grade decreases slowly, which means that this sensor has better detection precision at larger displacement. The characteristics of this sensor make sure that it could measure large displacement and has high detection accuracy at small displacement changes. The wavelength relative errors between experiment data and theory calculation results are all less than 5%. The relative error is bigger and bigger with the increase of external displacement. This phenomenon is mainly caused by machining technology of the prototype. With increasing the radius of gear, the depth of thread becomes smaller and smaller, which can be obtained from Fig.1. So the wavelength shifts in the experiment are always bigger than those in theory calculation. All these data confirm that this novel FBG displacement sensor has excellent measurement accuracy and achieves large range displacement detection.

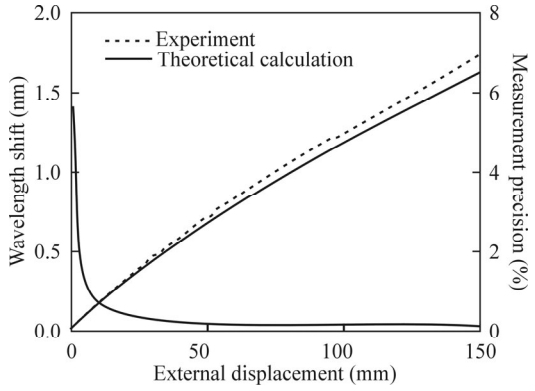

Fig.4 FBG center wavelength shift and measurement precision grade versus external displacement

In conclusion, with the mechanical transfer instrument of helical bevel gear, a novel FBG displacement sensor which can achieve high detection precision at small displacement changes and wide measurement range is proposed in this paper. Because the helical bevel gear has varying radius along with its axis, this sensor has varying detection accuracy. So the mutative precision grade is chosen as one reference index to identify its performance. The calculation model of this sensor is built, and the prototype is fabricated to confirm its performance practically. As geometrical and physical parameters are identified, the displacement detection range of this sensor is 0–1.751 m theoretically. Through analyzing the calibration experiment data, the detection accuracy range is 11.8–15.9 pm/mm corresponding to external displacement from 0 mm to 150 mm. The relative errors of wavelength shift between theoretical and experimental data are all less than 5%. All these theoretical calculation and experiment data confirm that this sensor has excellent practical application, especially in large scale engineering structure measurement.

References

[1] H. B. Wang and Z. H. Feng, Sensors and Actuators A: Physical **203**, 362 (2013).

[2] T. Yeom, T. W. Simon and M. Zhang, Sensors and Actuators A: Physical **176**, 99 (2012).

[3] H. M. Cao, Y. P. Chen and Z. D. Zhou, Sensors and Actuators A: Physical **136**, 580 (2007).

[4] C. F. Cao and S. Ibaraki, Precision Engineering **37**, 159 (2013).

[5] M. T. Barzi and M. J. Khanjani, Ocean Engineering **38**, 419 (2011).

[6] Fang Xie, Junyu Ren, Zhimin Chen and Qibo Feng, Optics and Laser Technology **42**, 208 (2010).

[7] A. Sun, Z. S. Wu and H. Huang, Optics Communications **311**, 140 (2013).

[8] D. S. Xu, J. H. Yin and Z. Zhen, Measurement **46**, 200 (2013).

[9] Y. N. Zhang, Y. Zhao and Q. Wang, Sensors and Actuators A: Physical **214**, 168 (2014).

[10] Y. Zhao, Z. Q. Li and Y. Dong, Optik **125**, 6287 (2014).

[11] Y. Zou, X. P. Dong and G. B. Lin, Journal of Lightwave Technology **30**, 337 (2012).

[12] J. Z. Su, Z. D. Fang and X. W. Cai, Chinese Journal of Aeronautics **26**, 1310 (2013).

[13] C. H. Lin and Z. H. Fong, Mechanism and Machine Theory **84**, 1 (2015).

[14] D. D. Wang, M. Cao and C. Li, Procedia Engineering **15**, 704 (2011).

[15] Z. Zhou, J. L. Li and S. W. Sun, Electr. Electronic Eng. China **2**, 92 (2007).

[16] H. Q. Yuan, J. Yuan and J. Du, Journal of Wuhan University of Technology (Materials Science Edition) **18**, 94 (2003).

[17] GUO Yong-xing, ZHANG Dong-sheng, ZHOU Zu-de, LI Li-tong and ZHU Fang-dong, Journal of Optoelectronics·Lasers **25**, 435 (2014). (in Chinese)

[18] JIANG Qi, SONG Jin-xue, GAO Fang-fang, LI Yi-bin, RONG Xue-wen and LIU Hong-bin, Journal of Optoelectronics·Lasers **25**, 2123 (2014). (in Chinese)

[19] ZHAO Hong-xia, CHENG Pei-hong, BAO Ji-long and BAO Lei, Journal of Optoelectronics·Lasers **25**, 1071 (2014). (in Chinese)

[20] H. Zhou, J. Q. Wen and X. Z. Zhang, Physics Procedia **56**, 1102 (2014).